Supporting Information

Hellman et al. 10.1073/pnas.1005998107

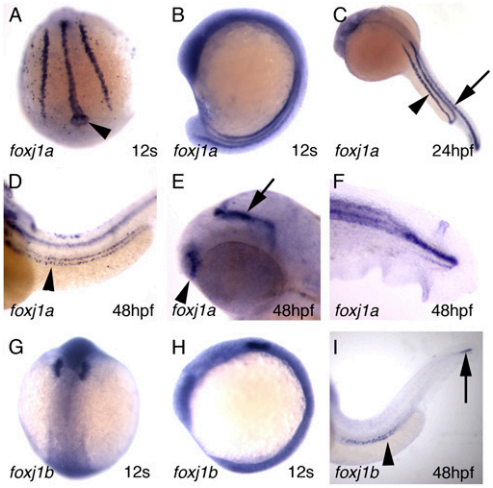

Fig. S1. *foxj1a* and *foxj1b* expression in ciliated cell types at different developmental stages. (*A* and *B*) *foxj1a* is uniformly expressed in precursors to the kidney and spinal cord at the 12-somite stage, as well as in Kupffer's vesicle (arrowhead). (*C*) At 24, hpf *foxj1a* is expressed throughout the spinal cord (arrow) and in all cells of the paired pronephric ducts (arrowhead). (*D*) By 48 hpf, *foxj1a* is down-regulated in singly ciliated cells of the pronephros but is maintained in a "salt-and-pepper" pattern in tubule cells, consistent with expression in multiciliated cells. (*E*) At 48 hpf, expression is also observed in the olfactory placode (arrowhead) and brain ventricular system (arrow). (*F*) Spinal cord is positive for *foxj1a* at 48 hpf. (*G* and *H*) *foxj1b* is expressed in developing otic placodes (arrowheads) at the 12-somite stage, and (*I*) in pronephric multiciliated cells (arrowhead) at 48 hpf. Note that *foxj1b* expression is seen only at the most distal tip of the spinal cord (arrow).

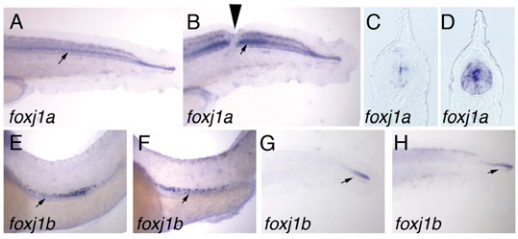

Fig. S2. In spinal cord injury, *foxj1a* but not *foxj1b* is up-regulated. (*A*) *foxj1a* is expressed in the developing spinal cord, and is up-regulated 8 h after mechanical cord injury (arrowhead) induced with a forceps (*B*). Histological sections of control spinal cord (*C*) and injured spinal cord (*D*) reveals an injury-mediated increase in *foxj1a* in ciliated spinal cord cells. In contrast, *foxj1b* gene expression remains restricted to multiciliated cells of the pronephric duct in both control (*E*) and obstructed (*F*) embryos, and likewise remains restricted to the distal tip of the spinal cord in both spinal cord-intact (*G*) and spinal cord-injured (*H*) embryos.

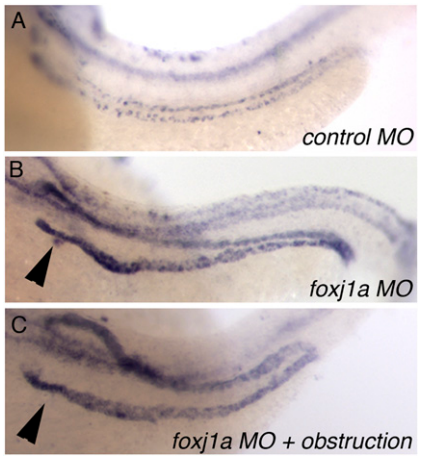

Fig. S3. Induction of *foxj1a* expression by obstruction does not require translation of *foxj1a* mRNA. (*A*) *foxj1a* expression in control 48 hpf embryos is concentrated in multiciliated cells and not in proximal tubule single ciliated cells. (*B*) *foxj1a* mRNA expression was up-regulated in *foxj1a* knockdown embryos (combination of ATG and splice donor-blocking morpholino oligos). (*C*) Knockdown of *foxj1a* translation did not prevent up-regulation of *foxj1a* mRNA by obstruction, arguing against an autoregulatory induction mechanism.

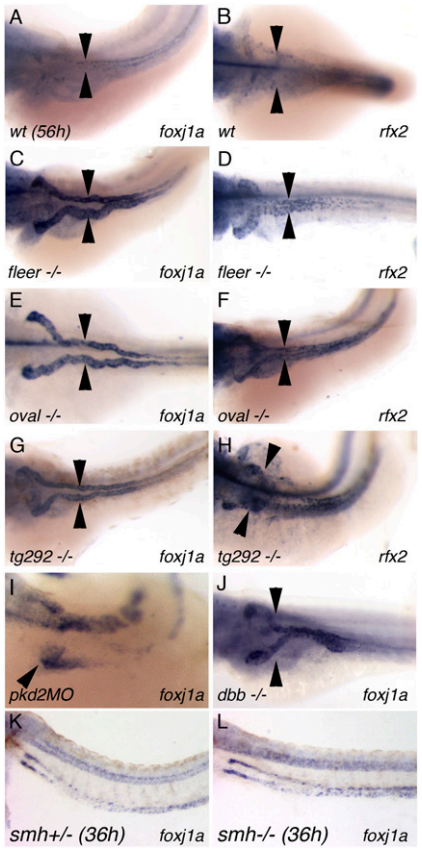

Fig. S4. *foxj1a* and *rfx2* are up-regulated in zebrafish cystic kidney mutants. (*A* and *B*) In WT embryos at 56 hpf, both *foxj1a* and *rfx2* were expressed in a "salt-and-pepper" distribution characteristic of multiciliated pronephric duct cells. Expression of *foxj1a* and *rfx2* was up-regulated in all cells of the pronephric duct in the dilated pronephric ducts (arrowheads) of 56-hpf embryos homozygous for *fleer* (*C* and *D*), *oval* (*E* and *F*), *tg292a* (*G* and *H*), and *double bubble* (*J*) mutations, all of which developed pronephric cysts by 56 hfp, as well as in *pkd2* morphants (*I*). No increase in *foxj1a* expression over control was observed in pronephros of mutants before cystic stretch (36 hpf,) shown here for the *schmalhans* cilia cystic mutant (*K* and *L*).

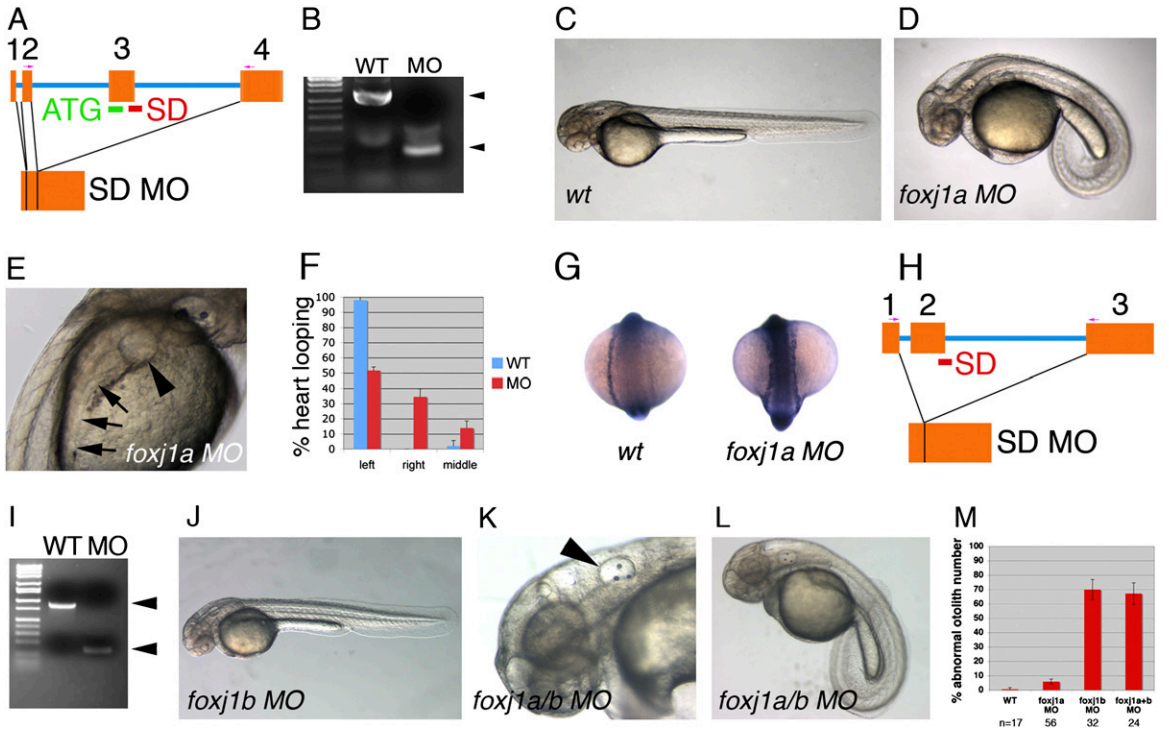

Fig. S5. *foxj1a* and *foxj1b* morphants exhibit distinct ciliopathy phenotypes. (*A*) Genomic structure of the zebrafish *foxj1a* gene and sites of ATG and splice donor (SD) MO used in this study. SD MO results in complete deletion of exon 3 as determined by sequencing. (*B*) RT-PCR analysis of control (WT) and *foxj1a* SD morphant embryo RNA, indicating complete loss of normal *foxj1a* mRNA induced by mis-splicing in *foxj1a* SD morphants. (*C*) Control morpholino-injected zebrafish at 48 hpf compared with (*D*) zebrafish injected with a mixture of both *foxj1a* ATG and SD MO, which uniformly exhibited ventrally curved body axis, hydrocephalus, and normal otolith number (two per otic placode), as well as (*E*) glomerular cysts (arrowhead) and dilated pronephric tubules (arrows). *foxj1a* morphants showed frequent *situs inversus*, as determined by assessment of heart-looping (*F*; error bars represent SD of three averaged experiments; $n = 98$ embryos total) and bilateral expression of *southpaw* (*G*). (*H*) Intron–exon boundaries for zebrafish *foxj1b* and the exon 2 SD MO target site. RT-PCR demonstrated complete loss of WT mRNA and deletion of exon 2 in *foxj1b* morphants (*I*). (*J*) *foxj1b* Morphants appeared relatively normal, with the exception of abnormal otolith number (*K*; arrowhead depicting otic placode with three otoliths present). (*L*) *foxj1a/b* double knockdown embryos demonstrate curved body axis, kidney cysts, hydrocephalus, and abnormal otolith number. (*M*) Quantification of abnormal otolith number in *foxj1a, foxj1b,* and *foxj1a+b* double morphants. Error bars represent standard deviation of three averaged experiments).

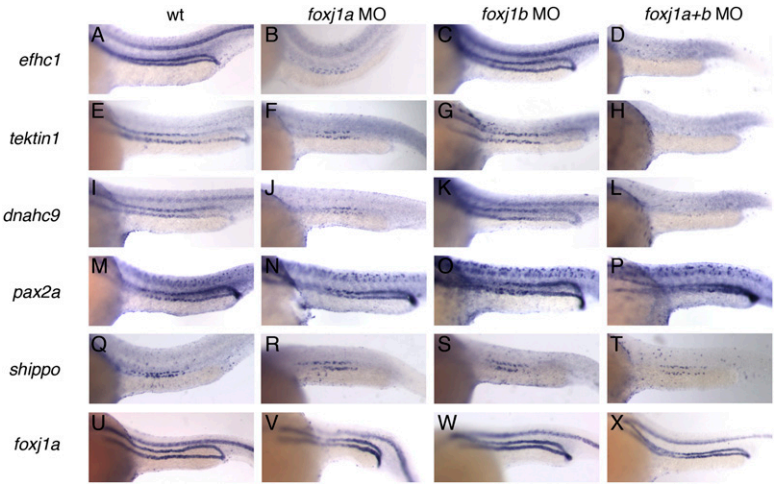

Fig. S6. *efhc1*, *tektin-1*, and *dnahc9* expression in the pronephros is *foxj1a* and *foxj1b* dependent. In situ hybridization analysis in control, *foxj1a* morphant (MO), *foxj1b* MO, and *foxj1a+b* double morphants at 24 hpf demonstrated that combined *foxj1a/b* double knockdown uniformly abolished expression of cilia motility associated genes but not other kidney specific markers or *foxj1a* itself. (*A–D*) EF-hand containing domain 1 (*efhc1*), (*E–H*) *tektin-1*, (*I–K*) dynein heavy chain 9 (*dnahc9*), (*M–P*) *pax2a*, (*Q–T*) shippo, (*U–X*) *foxj1a* ($n > 15$ embryos for each condition). (*A, E, I, M, Q, U*) Control embryos; (*B, F, J, N, R, V*) *foxj1a* MO; (*C, G, K, O, S, W*) *foxj1b* MO; (*D, H, L, P, T, X*) combined *foxj1a/b* knockdown.

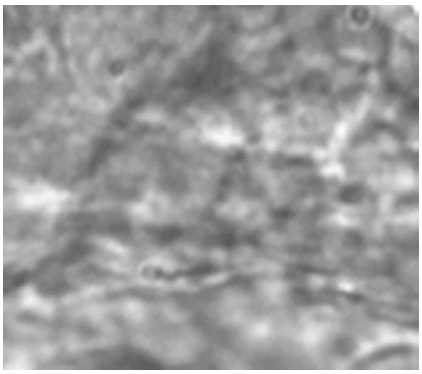

Movie S1. High-speed video microscopy showing a control, unobstructed pronephric duct in a 56-hpf embryo with a representative cilium beating at 48 beats/s (bps). The entire video represents 1 full s of real time slowed down to 6 frames/s, making it possible to manually count cilia beat rate.

Movie S1

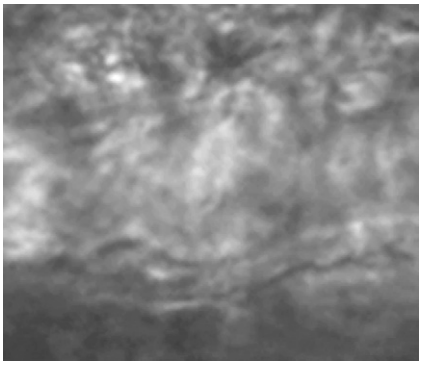

Movie S2. High-speed video microscopy showing a dilated pronephric duct following 3.5 h of mechanical obstruction, with a representative cilium beating at a rate of 67 beats/s.

Movie S2

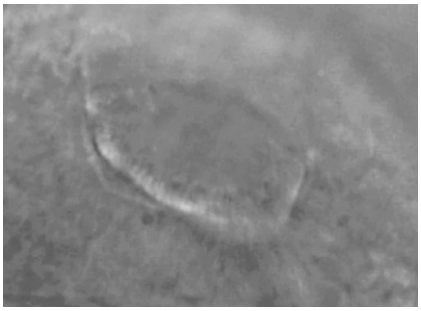

Movie S3. High-speed video microscopy showing control cilia of the olfactory placode at 56 hpf, demonstrating normal cilia motility.

Movie S3

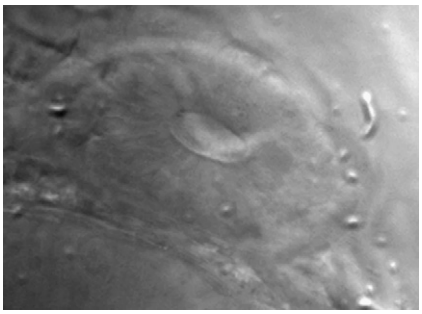

Movie S4. High-speed video microscopy of *foxj1a* morphant olfactory placode at 56 hpf, demonstrating an absence of motile cilia.

Movie S4

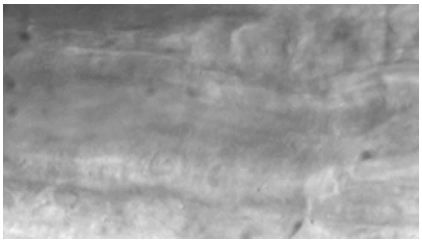

Movie S5. High-speed video microscopy of *foxj1a/b* morphant pronephric duct demonstrating an absence of motile cilia. Note that the pronephric duct is markedly dilated compared with the control pronephric duct in Movie S1.

Movie S5

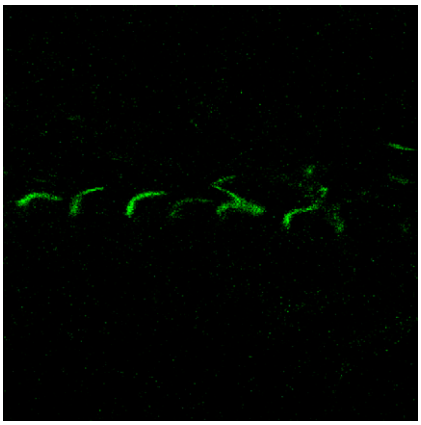

Movie S6. Time-lapse confocal microscopy demonstrating scorpion-eGFP (sco-eGFP)-labeled control spinal cord ependymal cilia that are motile.

Movie S6

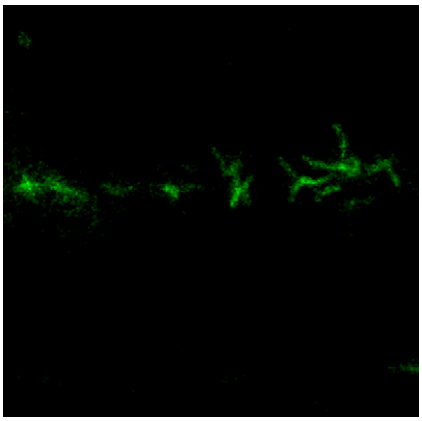

Movie S7. Time-lapse confocal microscopy demonstrating sco-eGFP–labeled *foxj1a* morphant spinal cord ependymal cilia that are immotile.

Movie S7